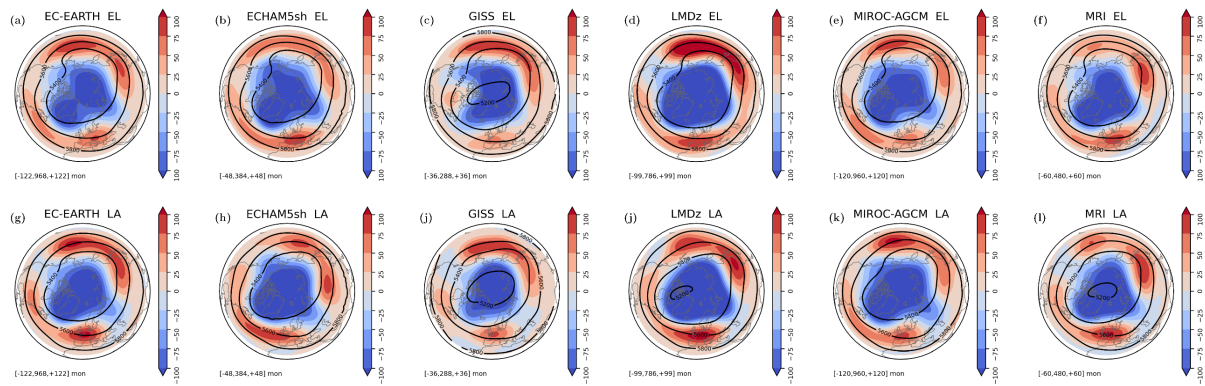


QBOi El Nino Southern Oscillation experiments: Teleconnections of the QBO

5 Naoe, Hiroaki¹, Jorge L. García-Franco², Chang-Hyun Park³, Mario Rodrigo⁴, Froila M. Palmeiro^{4,5},
Federico Serva⁶, Masakazu Taguchi⁷, Kohei Yoshida¹, James A. Anstey⁸, Javier García-Serrano^{4,9},
Seok-Woo Son³, Yoshio Kawatani¹⁰, Neal Butchart¹¹, Kevin Hamilton¹², Chih-Chieh Chen¹³, Anne
Glanville¹³, Tobias Kerzenmacher¹⁴, François Lott¹⁵, Clara Orbe¹⁶, Scott Osprey¹⁷, Mijeong Park¹³,
Jadwiga H. Richter¹³, Stefan Versick¹⁴, Shingo Watanabe¹⁸

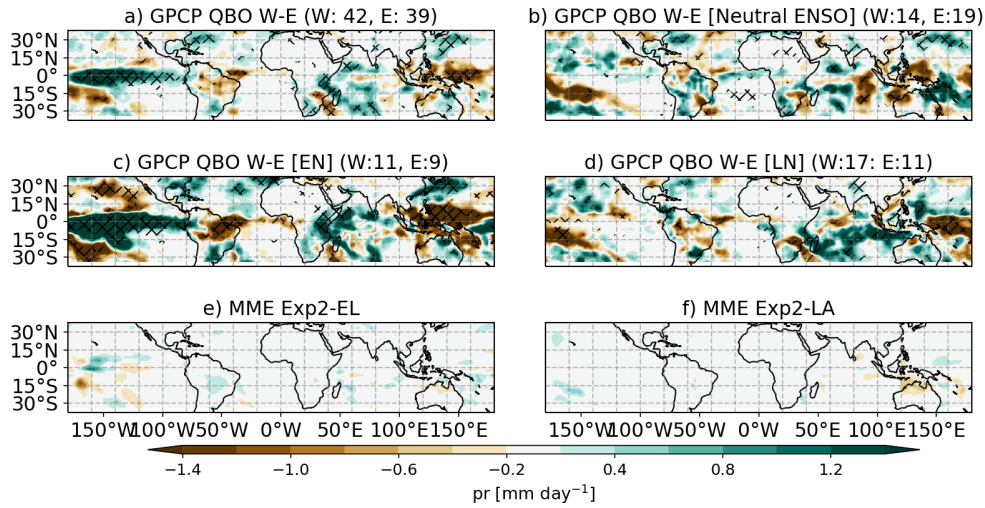
10

Supplement figures



20 **Figure S1: Northern annular mode stereographic maps at 500 hPa in EN and LN experiments for QBOi models based on their geopotential daily data. Contour lines indicate the geopotential height during neutral annular mode conditions. Colors are the positive (strong vortex, above the 90th percentile) minus negative (weak vortex, below the 10th percentile) anomalies based on the NAM index. Negative anomalies indicate lower geopotential heights.**

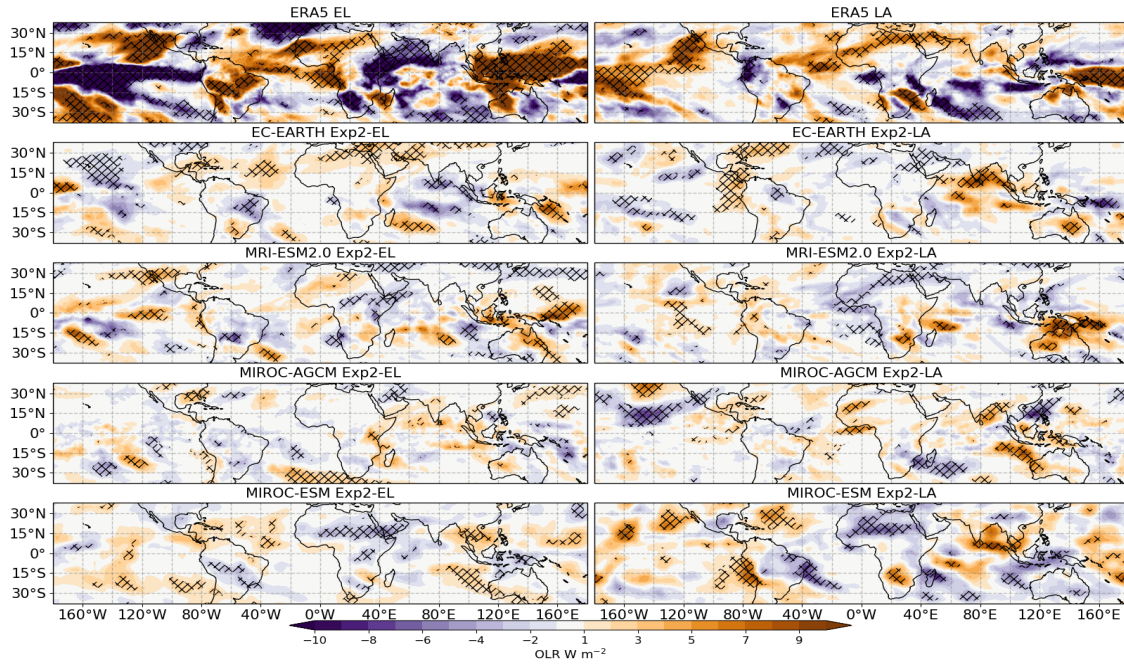
35



50

Figure S2. As in Figure 8 but showing the observed QBO signal for a) all DJF periods, and under b) Neutral, c) EN, d) or LA conditions. The QBOi models are composited into a multimodel-mean, regridded to a common grid (the GPCP grid), and MME differences are shown for the e) EN and (f) LN experiments. Model agreement, defined as grid-points where at least 75% of the models agree on the sign of the signal, are hatched. The observed composite sizes in months are shown in parenthesis in the GPCP panels.

55



80 **Figure S3:** As Fig. 8, but for outgoing longwave radiation (OLR) in W m^{-2} . ERA5 data are used as the observational benchmark. Only some models of the QBOi cohort output OLR for these experiments.

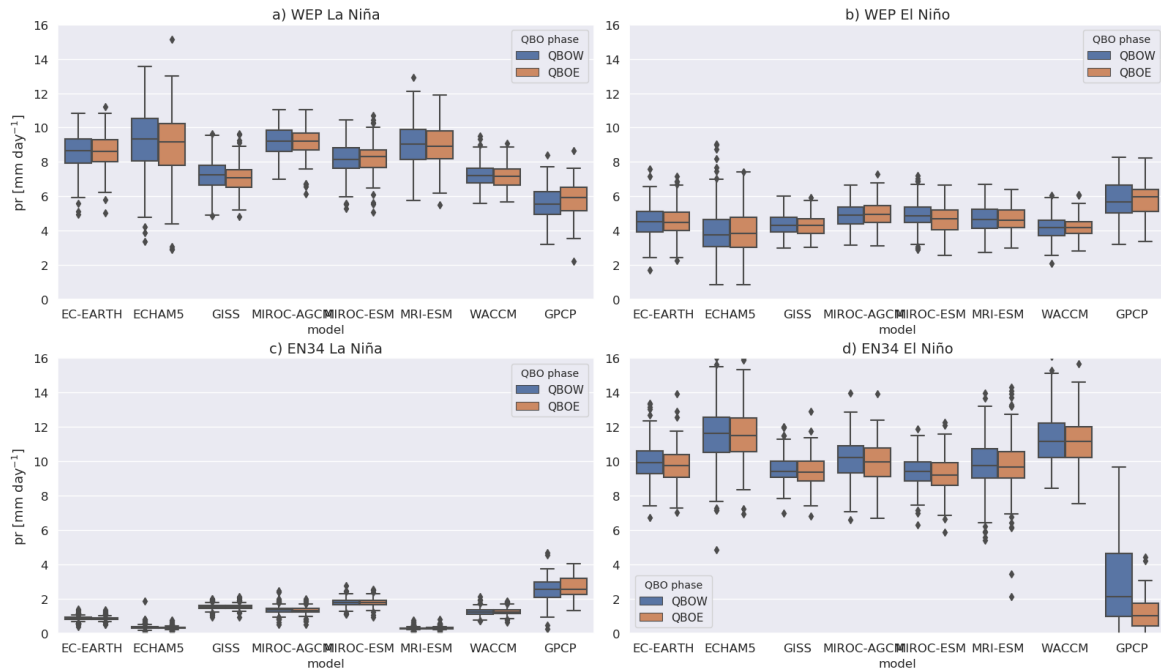
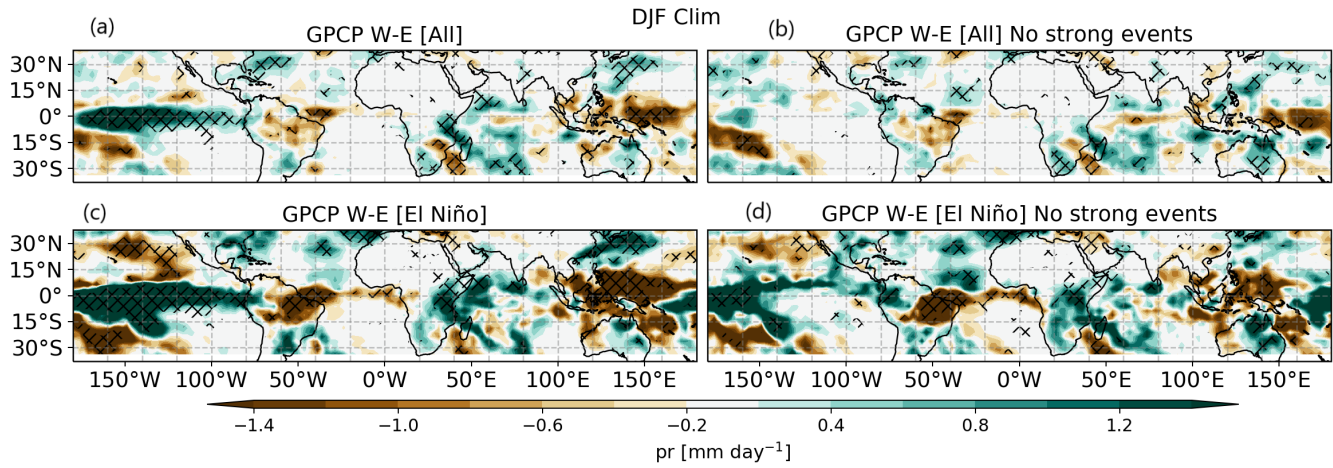
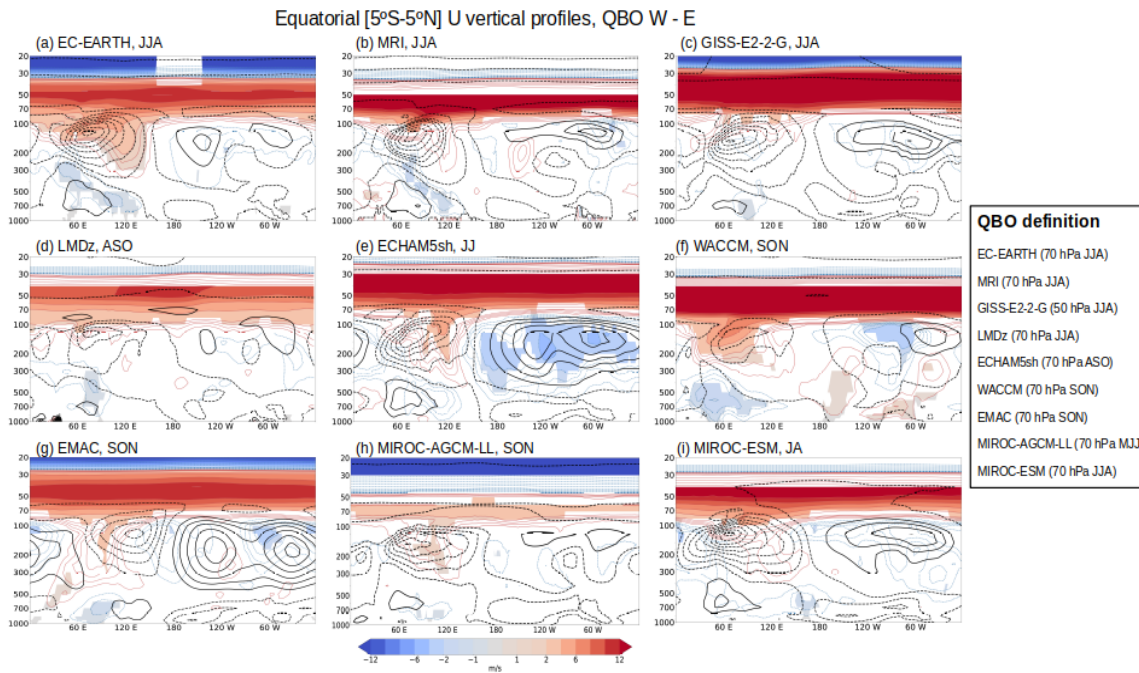


Figure S4: (Left) Box plots of deseasonalized precipitation (mm day^{-1}) averaged over the western equatorial Pacific (WEP) region (5° S – 5° N , 120° – 170° E) and EN3.4 region (5° S – 5° N , 170° – 120° W) for (a, c) LN and (b, d) EN experiments for the models, together with El Niño and La Niña years in GPCP data, separated by datasets and QBO phases. QBO phases are classified using deseasonalized DJF mean zonal-mean zonal wind averaged over 5° S – 5° N at 50 hPa using $\geq 2\text{ m s}^{-1}$ for QBO-W and $\leq -2\text{ m s}^{-1}$ for QBO-E.



100 **Figure S5. DJF composite differences in GPCP (1979-2021) for W-E QBO phases, considering (top) all winters and (bottom) only El Niño winters and (left) including the three strongest El Niño events or (right) removing them.**



130 **Figure S6:** Same as Figure 11, but for CTL experiments. Note that the EMAC model is included instead of ERA5, because we have not considered ENSO neutral years.

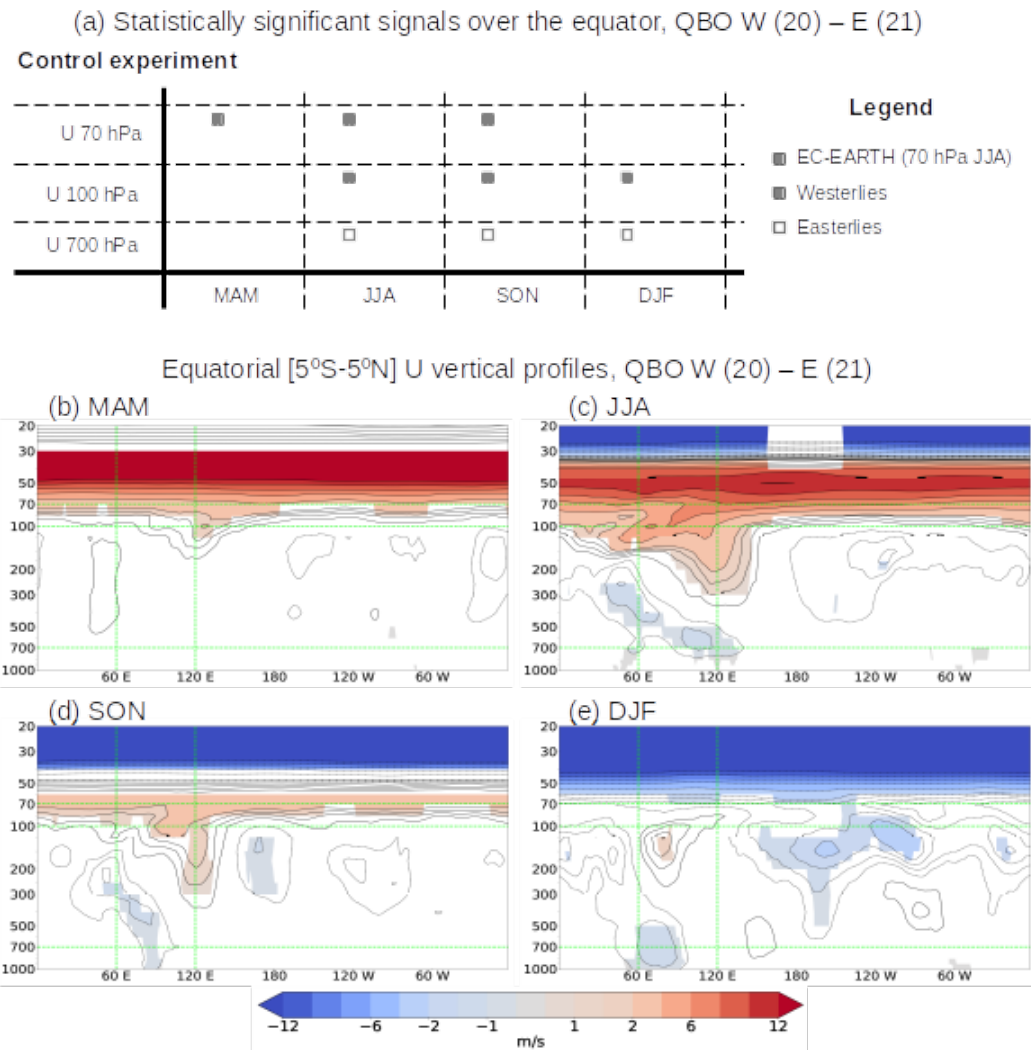


Figure S7: Schematic Hovmöller diagram showing statistically significant signals over the equator for the EC-EARTH CTL experiment (a). Westerly (W) minus Easterly (E) equatorial profiles of zonal wind for the EC-EARTH CTL experiment in MAM (b), JJA (c), SON (d), and DJF (e). Horizontal green dashed lines denote the vertical levels, while vertical lines mark the longitudinal regions used to complete the diagram in (a) for EC-EARTH.

165